# Energy Scan of the $e^+e^- \to h_b(nP)\pi^+\pi^-$ ($n = 1, 2$) Cross Sections and Evidence for $\Upsilon(11020)$ Decays into Charged Bottomoniumlike States

R. Mizuk,[31,40,41] A. Bondar,[3,50] I. Adachi,[13,9] H. Aihara,[68] D. M. Asner,[52] H. Atmacan,[38] V. Aulchenko,[3,50] T. Aushev,[41] R. Ayad,[61] I. Badhrees,[61,25] A. M. Bakich,[60] E. Barberio,[37] P. Behera,[17] V. Bhardwaj,[58] B. Bhuyan,[16] J. Biswal,[22] A. Bobrov,[3,50] G. Bonvicini,[73] A. Bozek,[47] M. Bračko,[35,22] T. E. Browder,[12] D. Červenkov,[4] V. Chekelian,[36] A. Chen,[44] B. G. Cheon,[11] K. Chilikin,[31,40] R. Chistov,[31,40] V. Chobanova,[36] S.-K. Choi,[10] Y. Choi,[59] D. Cinabro,[73] J. Dalseno,[36,63] M. Danilov,[40,31] N. Dash,[15] Z. Doležal,[4] A. Drutskoy,[31,40] S. Eidelman,[3,50] D. Epifanov,[68] T. Ferber,[6] B. G. Fulsom,[52] V. Gaur,[62] A. Garmash,[3,50] R. Gillard,[73] Y. M. Goh,[11] P. Goldenzweig,[24] B. Golob,[32,22] D. Greenwald,[64] T. Hara,[13,9] K. Hayasaka,[76] H. Hayashii,[43] W.-S. Hou,[46] C.-L. Hsu,[37] K. Inami,[42] G. Inguglia,[6] A. Ishikawa,[66] Y. Iwasaki,[13] I. Jaegle,[12] T. Julius,[37] K. H. Kang,[29] P. Katrenko,[41,31] D. Y. Kim,[57] H. J. Kim,[29] J. B. Kim,[27] K. T. Kim,[27] M. J. Kim,[29] S. H. Kim,[11] Y. J. Kim,[26] K. Kinoshita,[5] P. Kodyš,[4] S. Korpar,[35,22] D. Kotchetkov,[12] P. Krokovny,[3,50] T. Kuhr,[33] A. Kuzmin,[3,50] Y.-J. Kwon,[75] J. S. Lange,[8] C. H. Li,[37] H. Li,[18] L. Li,[54] L. Li Gioi,[36] J. Libby,[17] D. Liventsev,[72,13] M. Lubej,[22] T. Luo,[53] M. Masuda,[67] T. Matsuda,[39] D. Matvienko,[3,50] K. Miyabayashi,[43] H. Miyata,[49] G. B. Mohanty,[62] A. Moll,[36,63] E. Nakano,[51] M. Nakao,[13,9] T. Nanut,[22] K. J. Nath,[16] K. Negishi,[66] M. Niiyama,[28] N. K. Nisar,[62,1] S. Nishida,[13,9] S. Ogawa,[65] S. Okuno,[23] S. L. Olsen,[55] Y. Onuki,[68] P. Pakhlov,[31,40] G. Pakhlova,[31,41] B. Pal,[5] C. W. Park,[59] H. Park,[29] S. Paul,[64] T. K. Pedlar,[34] R. Pestotnik,[22] M. Petrič,[22] L. E. Piilonen,[72] C. Pulvermacher,[24] M. Ritter,[33] Y. Sakai,[13,9] S. Sandilya,[5] T. Sanuki,[66] V. Savinov,[53] T. Schlüter,[33] O. Schneider,[30] G. Schnell,[2,14] C. Schwanda,[20] Y. Seino,[49] D. Semmler,[8] K. Senyo,[74] O. Seon,[42] M. E. Sevior,[37] V. Shebalin,[3,50] T.-A. Shibata,[69] J.-G. Shiu,[46] B. Shwartz,[3,50] F. Simon,[36,63] E. Solovieva,[31,41] M. Starič,[22] J. Stypula,[47] T. Sumiyoshi,[70] M. Takizawa,[56] U. Tamponi,[21,71] K. Tanida,[55] Y. Teramoto,[51] I. Tikhomirov,[40] K. Trabelsi,[13,9] M. Uchida,[69] T. Uglov,[31,41] Y. Unno,[11] S. Uno,[13,9] P. Urquijo,[37] Y. Usov,[3,50] C. Van Hulse,[2] G. Varner,[12] V. Vorobyev,[3,50] C. H. Wang,[45] M.-Z. Wang,[46] P. Wang,[19] X. L. Wang,[72] Y. Watanabe,[23] K. M. Williams,[72] E. Won,[27] J. Yamaoka,[52] Y. Yamashita,[48] J. Yelton,[7] C. Z. Yuan,[19] Z. P. Zhang,[54] V. Zhilich,[3,50] V. Zhukova,[40] V. Zhulanov,[3,50] and A. Zupanc[32,22]

(Belle Collaboration)

[1]*Aligarh Muslim University, Aligarh 202002*
[2]*University of the Basque Country UPV/EHU, 48080 Bilbao*
[3]*Budker Institute of Nuclear Physics SB RAS, Novosibirsk 630090*
[4]*Faculty of Mathematics and Physics, Charles University, 121 16 Prague*
[5]*University of Cincinnati, Cincinnati, Ohio 45221*
[6]*Deutsches Elektronen-Synchrotron, 22607 Hamburg*
[7]*University of Florida, Gainesville, Florida 32611*
[8]*Justus-Liebig-Universität Gießen, 35392 Gießen*
[9]*SOKENDAI (The Graduate University for Advanced Studies), Hayama 240-0193*
[10]*Gyeongsang National University, Chinju 660-701*
[11]*Hanyang University, Seoul 133-791*
[12]*University of Hawaii, Honolulu, Hawaii 96822*
[13]*High Energy Accelerator Research Organization (KEK), Tsukuba 305-0801*
[14]*IKERBASQUE, Basque Foundation for Science, 48013 Bilbao*
[15]*Indian Institute of Technology, Bhubaneswar, Satya Nagar 751007*
[16]*Indian Institute of Technology, Guwahati, Assam 781039*
[17]*Indian Institute of Technology, Madras, Chennai 600036*
[18]*Indiana University, Bloomington, Indiana 47408*
[19]*Institute of High Energy Physics, Chinese Academy of Sciences, Beijing 100049*
[20]*Institute of High Energy Physics, Vienna 1050*
[21]*INFN—Sezione di Torino, 10125 Torino*
[22]*J. Stefan Institute, 1000 Ljubljana*
[23]*Kanagawa University, Yokohama 221-8686*
[24]*Institut für Experimentelle Kernphysik, Karlsruher Institut für Technologie, 76131 Karlsruhe*
[25]*King Abdulaziz City for Science and Technology, Riyadh 11442*
[26]*Korea Institute of Science and Technology Information, Daejeon 305-806*
[27]*Korea University, Seoul 136-713*
[28]*Kyoto University, Kyoto 606-8502*

 

[29]Kyungpook National University, Daegu 702-701
[30]École Polytechnique Fédérale de Lausanne (EPFL), Lausanne 1015
[31]P. N. Lebedev Physical Institute of the Russian Academy of Sciences, Moscow 119991
[32]Faculty of Mathematics and Physics, University of Ljubljana, 1000 Ljubljana
[33]Ludwig Maximilians University, 80539 Munich
[34]Luther College, Decorah, Iowa 52101
[35]University of Maribor, 2000 Maribor
[36]Max-Planck-Institut für Physik, 80805 München
[37]School of Physics, University of Melbourne, Victoria 3010
[38]Middle East Technical University, 06531 Ankara
[39]University of Miyazaki, Miyazaki 889-2192
[40]Moscow Physical Engineering Institute, Moscow 115409
[41]Moscow Institute of Physics and Technology, Moscow Region 141700
[42]Graduate School of Science, Nagoya University, Nagoya 464-8602
[43]Nara Women's University, Nara 630-8506
[44]National Central University, Chung-li 32054
[45]National United University, Miao Li 36003
[46]Department of Physics, National Taiwan University, Taipei 10617
[47]H. Niewodniczanski Institute of Nuclear Physics, Krakow 31-342
[48]Nippon Dental University, Niigata 951-8580
[49]Niigata University, Niigata 950-2181
[50]Novosibirsk State University, Novosibirsk 630090
[51]Osaka City University, Osaka 558-8585
[52]Pacific Northwest National Laboratory, Richland, Washington 99352
[53]University of Pittsburgh, Pittsburgh, Pennsylvania 15260
[54]University of Science and Technology of China, Hefei 230026
[55]Seoul National University, Seoul 151-742
[56]Showa Pharmaceutical University, Tokyo 194-8543
[57]Soongsil University, Seoul 156-743
[58]University of South Carolina, Columbia, South Carolina 29208
[59]Sungkyunkwan University, Suwon 440-746
[60]School of Physics, University of Sydney, New South Wales 2006
[61]Department of Physics, Faculty of Science, University of Tabuk, Tabuk 71451
[62]Tata Institute of Fundamental Research, Mumbai 400005
[63]Excellence Cluster Universe, Technische Universität München, 85748 Garching
[64]Department of Physics, Technische Universität München, 85748 Garching
[65]Toho University, Funabashi 274-8510
[66]Department of Physics, Tohoku University, Sendai 980-8578
[67]Earthquake Research Institute, University of Tokyo, Tokyo 113-0032
[68]Department of Physics, University of Tokyo, Tokyo 113-0033
[69]Tokyo Institute of Technology, Tokyo 152-8550
[70]Tokyo Metropolitan University, Tokyo 192-0397
[71]University of Torino, 10124 Torino
[72]Virginia Polytechnic Institute and State University, Blacksburg, Virginia 24061
[73]Wayne State University, Detroit, Michigan 48202
[74]Yamagata University, Yamagata 990-8560
[75]Yonsei University, Seoul 120-749
[76]Kobayashi-Maskawa Institute, Nagoya University, Nagoya 464-8602
(Received 7 June 2016; published 28 September 2016)

Using data collected with the Belle detector at the KEKB asymmetric-energy $e^+e^-$ collider, we measure the energy dependence of the $e^+e^- \to h_b(nP)\pi^+\pi^-$ ($n = 1, 2$) cross sections from thresholds up to 11.02 GeV. We find clear $\Upsilon(10860)$ and $\Upsilon(11020)$ peaks with little or no continuum contribution. We study the resonant substructure of the $\Upsilon(11020) \to h_b(nP)\pi^+\pi^-$ transitions and find evidence that they proceed entirely via the intermediate isovector states $Z_b(10610)$ and $Z_b(10650)$. The relative fraction of these states is loosely constrained by the current data: The hypothesis that only $Z_b(10610)$ is produced is excluded at the level of 3.3 standard deviations, while the hypothesis that only $Z_b(10650)$ is produced is not excluded at a significant level.

DOI: 10.1103/PhysRevLett.117.142001

Heavy quarkonia are the bound states of $c\bar{c}$ or $b\bar{b}$ quarks. In such states, the quarks are moving relatively slowly, and therefore a nonrelativistic approximation based on the interaction potential accurately describes the basic properties of the system [1]. The first state that did not fit potential model expectations was observed in 2003 by Belle [2]; since then, nearly 20 such states have been reported [3]. All these states correspond to high excitations and have masses above the $D\bar{D}$ or $B\bar{B}$ thresholds.

Many quarkoniumlike states were found in the energy scans of the cross sections of $e^+e^-$ annihilation into conventional quarkonia and light hadrons. Among these are the $Y(4008)$ and $Y(4260)$ in $J/\psi\pi^+\pi^-$ [4], the $Y(4360)$ and $Y(4660)$ in $\psi(2S)\pi^+\pi^-$ [5], the $\psi(4040)$ and $\psi(4160)$ in $J/\psi\eta$ [6], and possibly the $Y(4220)$ in $h_c\pi^+\pi^-$ [7]. The partial widths of the corresponding transitions are much higher than expected for conventional quarkonia [8]. Surprisingly, the peaks observed in the cross sections depend on the final states. In other words, each such charmoniumlike state decays to only one channel with charmonium. To explain this "selectivity," a hadrocharmonium notion is introduced [9]: a bound state of a charmonium and a light hadron. Such a system decays predominantly into its constituents.

Recent energy scans of the $e^+e^- \to \Upsilon(nS)\pi^+\pi^-$ ($n = 1$, 2, 3) cross sections by Belle [10,11] show that the situation is different in the sector of bottomoniumlike states: All of the cross sections exhibit peaks of the $\Upsilon(10860)$ and $\Upsilon(11020)$ resonances that are also seen in the total hadronic cross section. The observed decay patterns of $\Upsilon(10860)$ and $\Upsilon(11020)$ agree with the expectations for a mixture of the $B_{(s)}^{(*)}\bar{B}_{(s)}^{(*)}$ molecule and conventional bottomonium: Open flavor channels dominate, while channels with quarkonium have anomalously high partial widths [12]. The striking difference between charmoniumlike and bottomoniumlike states, that we describe above, is not yet understood. Further scans in the bottomonium region are therefore of high importance. In this Letter, we report the first energy scan of the $e^+e^- \to h_b(nP)\pi^+\pi^-$ ($n = 1, 2$) cross sections. We find clear $\Upsilon(10860)$ and $\Upsilon(11020)$ peaks without a significant continuum contribution.

To date, the $e^+e^- \to h_b(nP)\pi^+\pi^-$ processes were seen only at a single energy near the $\Upsilon(10860)$ peak [13]. They were found to proceed entirely via the intermediate isovector states $Z_b(10610)$ and $Z_b(10650)$ that are situated near the $B\bar{B}^*$ and $B^*\bar{B}^*$ thresholds [14] and likely have corresponding molecular structures [15]. Here, we report on the resonant substructure study of the $\Upsilon(11020) \to h_b(nP)\pi^+\pi^-$ decays, where we find the first evidence for intermediate $Z_b$ states. Hereinafter, the $\Upsilon(10860)$ and $\Upsilon(11020)$ are referred to, for brevity, as the $\Upsilon(5S)$ and $\Upsilon(6S)$ according to the potential model assignment.

We use 121.4 $\mathrm{fb}^{-1}$ of on-resonance $\Upsilon(5S)$ data taken at three energies close to 10.866 GeV, as well as 1 $\mathrm{fb}^{-1}$ of data taken at each of 19 different energies between 10.77 and 11.02 GeV. These data were collected with the Belle detector [16] at the KEKB asymmetric-energy $e^+e^-$ collider [17].

The $e^+e^- \to h_b(nP)\pi^+\pi^-$ processes are reconstructed inclusively based on the $\pi^+\pi^-$ missing mass $M_{\mathrm{miss}}(\pi\pi) = \sqrt{(E_{\mathrm{c.m.}} - E^*_{\pi\pi})^2 - p^{*2}_{\pi\pi}}$, where $E_{\mathrm{c.m.}}$ is the center-of-mass (c.m.) energy and $E^*_{\pi\pi}$ and $p^*_{\pi\pi}$ are the energy and momentum, respectively, of the $\pi^+\pi^-$ pair as measured in the c.m. frame. The c.m. energy is calibrated using the $e^+e^- \to \Upsilon(nS)\pi^+\pi^- \to \mu^+\mu^-\pi^+\pi^-$ and $e^+e^- \to \mu^+\mu^-$ processes, as described in Ref. [11]. This analysis closely follows those of previous Belle publications [13,14,18].

We use a general hadronic event selection with requirements on the position of the primary vertex, track multiplicity (more than two tracks), and the total energy and momentum of the event [19]. These criteria suppress Bhabha, $\mu^+\mu^-$, $\tau^+\tau^-$, two-photon, and beam-gas processes. Continuum $e^+e^- \to q\bar{q}$ ($q = u, d, s, c$) events have jetlike shapes in contrast to the spherically symmetric signal events and are suppressed by a requirement on the ratio of the second-to-zeroth Fox-Wolfram moments: $R_2 < 0.3$ [20]. We consider only positively identified $\pi^+\pi^-$ candidates that originate from the interaction point region.

The measurements of the cross sections are performed with an additional requirement on the *single-pion* $\pi^\pm$ missing mass:

$$10.59\ \mathrm{GeV}/c^2 < M_{\mathrm{miss}}(\pi^\pm) < 10.67\ \mathrm{GeV}/c^2, \qquad (1)$$

which selects signal events proceeding via the intermediate $Z_b(10610)$ or $Z_b(10650)$ states. We combine the $M_{\mathrm{miss}}(\pi\pi)$ distribution for $\pi^+$ satisfying (1) and that for $\pi^-$ satisfying (1). The $\pi^+\pi^-$ pairs with both $M_{\mathrm{miss}}(\pi^+)$ and $M_{\mathrm{miss}}(\pi^-)$ in the $Z_b$ mass window are counted twice. [If they are counted only once, the combinatorial background develops a dip slightly above the $h_b(2P)$ signal, making the background parameterization difficult.] We take the double entries into account by correcting the errors of the $M_{\mathrm{miss}}(\pi\pi)$ histogram and, based on Monte Carlo (MC) simulation, the $h_b(2P)$ signal yields.

We fit the $M_{\mathrm{miss}}(\pi\pi)$ distribution in the $h_b(1P)$ and $h_b(2P)$ intervals, defined as 9.8–10.0 and 10.17–10.34 $\mathrm{GeV}/c^2$, respectively. The fit function is the sum of the $h_b(nP)$ signal and combinatorial- and peaking-background components. The shapes of the $h_b(nP)$ signals are determined by convolving the probability density of the initial state radiation (ISR) process with the experimental resolution, described by a Gaussian. We use the ISR probability, calculated up to the second order [21], and take into account the energy dependence of the $e^+e^- \to h_b(nP)\pi^+\pi^-$ cross sections using an iterative procedure. The resolution is determined using the exclusively reconstructed decays $\Upsilon(5S) \to \Upsilon(nS)\pi^+\pi^-$, $\Upsilon(nS) \to \mu^+\mu^-$ to be $(6.84 \pm 0.13)\ \mathrm{MeV}/c^2$ for the

$h_b(1P)$ and $(6.15 \pm 0.22)$ MeV$/c^2$ for the $h_b(2P)$. The resolution is dominated by c.m. energy smearing. The $h_b(nP)$ masses are fixed at the previous Belle measurement [18]. We normalize the signal density functions in such a way that the measured $h_b(nP)$ yields include the ISR correction $1 + \delta_{\rm ISR}$ and can be used directly to measure the Born cross sections. The combinatorial background is described by a fourth-order Chebyshev polynomial in both fit intervals. The order is chosen by maximizing the confidence level of the fit.

Using MC simulation, we find that combining a random pion that satisfies the $Z_b$ mass requirement and a signal pion from $Z_b \to h_b(nP)\pi$ produces a broad bump under the $h_b(nP)$ signal. This background is absorbed in the polynomial of the combinatorial background and results in minor corrections in the $h_b(1P)$ and $h_b(2P)$ yields of $0.99 \pm 0.01$ and $0.995 \pm 0.005$, respectively. The $\pi^+\pi^-$ pairs originating from the $\Upsilon(2S) \to \Upsilon(1S)\pi^+\pi^-$ transitions with the $\Upsilon(2S)$ produced inclusively or via ISR result in a peak at $E_{\rm c.m.} - [m_{\Upsilon(2S)} - m_{\Upsilon(1S)}]$ that is inside the $h_b(2P)$ fit interval for the c.m. energies close to the $\Upsilon(5S)$. The shape of this peaking background is found from exclusively reconstructed $\Upsilon(1S) \to \mu^+\mu^-$ data to be a Gaussian with $\sigma = 11$ MeV$/c^2$. Its normalization is floated in the fit.

To determine the reconstruction efficiency, we use phase-space-generated MC events, weighted in $M_{\rm miss}(\pi)$ according to the fit results for the $\Upsilon(5S) \to h_b(1P)\pi^+\pi^-$ transitions [14] and in angular variables according to the expectations for the $Z_b$ spin parity $J^P = 1^+$ [22]. The efficiencies for the $h_b(1P)\pi^+\pi^-$ and $h_b(2P)\pi^+\pi^-$ channels are in the range 40%–55% and 35%–50%, respectively; they rise with c.m. energy. At the lowest energy point, there is a drop of efficiency by a factor of 2, since this point is close to the kinematic boundary and the pion momenta are low.

At each energy, the Born cross section is determined according to the formula

$$\sigma^B(e^+e^- \to h_b(nP)\pi^+\pi^-) = \frac{N}{L\varepsilon|1-\Pi|^2}, \qquad (2)$$

where $N$ is the number of signal events determined from the $M_{\rm miss}(\pi\pi)$ fit that includes the ISR correction, $L$ is the integrated luminosity, $\varepsilon$ is the reconstruction efficiency, and $|1-\Pi|^2$ is the vacuum polarization correction [23], which is in the range 0.927–0.930. The resulting cross sections are shown in Fig. 1. The cross sections, averaged over the three high statistics on-resonance points at $E_{\rm c.m.} = (10865.6 \pm 2.0)$ MeV, are

$$\sigma^B(e^+e^- \to h_b(1P)\pi^+\pi^-) = 1.66 \pm 0.09 \pm 0.10 \text{ pb}, \qquad (3)$$

$$\sigma^B(e^+e^- \to h_b(2P)\pi^+\pi^-) = 2.70 \pm 0.17 \pm 0.19 \text{ pb}. \qquad (4)$$

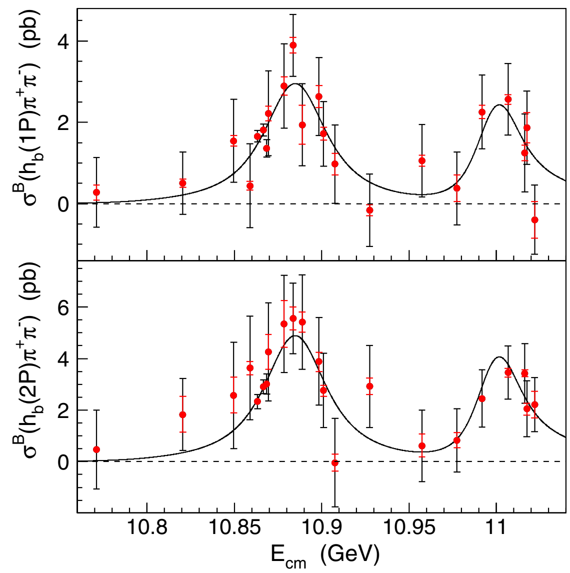


FIG. 1. The cross sections for the $e^+e^- \to h_b(1P)\pi^+\pi^-$ (top) and $e^+e^- \to h_b(2P)\pi^+\pi^-$ (bottom) as functions of c.m. energy. Points with error bars are the data; outer error bars indicate statistical uncertainties, and inner red error bars indicate uncorrelated systematic uncertainties. The solid curves are the fit results.

The ratio of the cross sections is $0.616 \pm 0.052 \pm 0.017$. Here and elsewhere in this Letter, the first uncertainties are statistical and the second are systematic.

The systematic uncertainties in the signal yields originate from the signal and background shapes. The uncertainties due to the $h_b(nP)$ masses and ISR tail shapes are found to be negligible. The relative uncertainty due to the $M_{\rm miss}(\pi\pi)$ resolution is correlated among different energy points and is equal to 1.4% for the $h_b(1P)$ and 3.3% for the $h_b(2P)$. The background-shape contribution is the only uncorrelated systematic uncertainty. It is estimated by varying the fit interval limits by about 50 MeV and the polynomial order for each fit interval. The corresponding uncertainties are 1.1% and 2.5% for the on-resonance cross sections in Eqs. (3) and (4), respectively.

A relative uncertainty in the efficiency contributes to the correlated systematic uncertainty. An uncertainty due to the $Z_b$ mass requirement of $^{+1.0}_{-1.8}\%$ is estimated by varying the $Z_b$ parameters by $\pm 1\sigma$ and taking into account correlations among different parameters. The efficiency of the $R_2$ requirement is studied using inclusively reconstructed $\Upsilon(5S) \to \Upsilon(nS)\pi^+\pi^-$ decays. We find good agreement between data and MC simulation and assign the 5% statistical uncertainty in the data as a systematic uncertainty due to the $R_2$ requirement. Finally, we assign a 1% uncertainty per track due to possible differences in the reconstruction efficiency between the data and MC simulation.

An uncertainty in the luminosity of 1.4% is primarily due to the simulation of Bhabha scattering that is used for its determination and is correlated among energy points. We add in quadrature all the contributions to find the total systematic uncertainties shown in Eqs. (3) and (4). The values of the cross sections for all energy points are provided in Ref. [24].

The shapes of the $h_b(1P)\pi^+\pi^-$ and $h_b(2P)\pi^+\pi^-$ cross sections look very similar. They show clear $\Upsilon(5S)$ and $\Upsilon(6S)$ peaks without significant continuum contributions. We perform a simultaneous fit of the shapes, adding in quadrature the statistical and uncorrelated systematic uncertainties at each energy point. We use the coherent sum of two Breit-Wigner amplitudes:

$$A_n \Phi_n(s) |F_{\rm BW}(s, M_5, \Gamma_5) + a e^{i\phi} F_{\rm BW}(s, M_6, \Gamma_6)|^2, \quad (5)$$

where $s \equiv E^2_{\rm c.m.}$, $\Phi_n(s)$ is the phase space calculated numerically, taking into account the measured $Z_b$ line shape [14], and $F_{\rm BW}(s, M, \Gamma) = M\Gamma/(s - M^2 + iM\Gamma)$ is a Breit-Wigner amplitude. The fit parameters $M_5, \Gamma_5, M_6, \Gamma_6$, $a$, and $\phi$ are common for the two channels, while only the normalization coefficients $A_n$ are different. Equation (5) is convolved with the $E_{\rm c.m.}$ resolution of $(5.0 \pm 0.4)$ MeV, which is found using exclusively reconstructed $\Upsilon(5S) \to \Upsilon(nS)\pi^+\pi^-$ events. The fitted functions are shown in Fig. 1. The confidence level of the fit is 93%. The fit results are

$$M_5 = (10884.7^{+3.6}_{-3.4}{}^{+8.9}_{-1.0})\ {\rm MeV}/c^2, \quad (6)$$

$$\Gamma_5 = (40.6^{+12.7}_{-8.0}{}^{+1.1}_{-19.1})\ {\rm MeV}, \quad (7)$$

$$M_6 = (10999.0^{+7.3}_{-7.8}{}^{+16.9}_{-1.0})\ {\rm MeV}/c^2, \quad (8)$$

$$\Gamma_6 = (27^{+27}_{-11}{}^{+5}_{-12})\ {\rm MeV}, \quad (9)$$

$$a = 0.65^{+0.36}_{-0.12}{}^{+0.17}_{-0.10}, \quad \text{and} \quad \phi = (0.1^{+0.4}_{-0.8} \pm 0.3)\pi. \quad (10)$$

The measured masses and widths agree with the results of the $\Upsilon(nS)\pi^+\pi^-$ scan [11].

The first error in the fit results is not purely statistical but includes uncorrelated systematic uncertainties in the cross sections. The contributions of other considered sources are listed in Table I.

TABLE I. The systematic uncertainties in the $\Upsilon(5S)$ and $\Upsilon(6S)$ masses (in MeV/$c^2$), widths (in MeV), amplitude $a$, and phase $\phi$ (in units of $\pi$).

| | $M_5$ | $\Gamma_5$ | $M_6$ | $\Gamma_6$ | $a$ | $\phi$ |
|---|---|---|---|---|---|---|
| Fit model | $^{+8.9}_{-0.1}$ | $^{+0.4}_{-19.1}$ | $^{+16.7}_{-0.0}$ | $^{+0.0}_{-11.5}$ | $^{+0.12}_{-0.00}$ | $^{+0.09}_{-0.00}$ |
| $Z_b$ substructure | $^{+0.2}_{-0.0}$ | $^{+0.0}_{-0.2}$ | $^{+0.1}_{-0.0}$ | $^{+0.7}_{-0.0}$ | $^{+0.11}_{-0.00}$ | $^{+0.00}_{-0.29}$ |
| $\sqrt{s}$ scale | 1.0 | 1.0 | $^{+3.0}_{-1.0}$ | $^{+4.7}_{-1.0}$ | $^{+0.00}_{-0.10}$ | $^{+0.25}_{-0.00}$ |
| Resolution | 0.0 | $^{+0.3}_{-0.2}$ | 0.1 | 0.6 | 0.0 | $^{+0.01}_{-0.00}$ |
| Total | $^{+8.9}_{-1.0}$ | $^{+1.1}_{-19.1}$ | $^{+16.9}_{-1.0}$ | $^{+4.8}_{-11.5}$ | $^{+0.17}_{-0.10}$ | $^{+0.27}_{-0.29}$ |

To study systematic uncertainties due to the fit model, we introduce a nonresonant continuum amplitude, $be^{i\delta}$. The significance of this contribution is only $1.6\sigma$. However, the shifts in the fit results are large, and this is the dominant source of systematic uncertainty. We also consider the possibility that the parameters $a$ and $\phi$ are different in the $h_b(1P)\pi^+\pi^-$ and $h_b(2P)\pi^+\pi^-$ channels. We find that the values in the two channels agree and the shifts in masses and widths are small. Using MC pseudoexperiments, we find that there is no significant fit bias.

If the resonant substructures of the $\Upsilon(5S)$ and $\Upsilon(6S)$ decays are different, the $\Upsilon(5S)$ and $\Upsilon(6S)$ amplitudes in Eq. (5) are not fully coherent, and the interference term is suppressed by a decoherence factor $k$ [11]. If only $Z_b(10610)$ is produced at the $\Upsilon(6S)$, $k$ is calculated numerically to be 0.62; if only $Z_b(10650)$ is produced, $k$ is 0.80. We introduce these factors in the fit and take into account that the efficiency of the $Z_b$ mass requirement is smaller for a single $Z_b$ state compared to two $Z_b$ states by 12%, since the two $Z_b$ states interfere destructively outside their signal region.

We account for an uncertainty in the $E_{\rm c.m.}$ scale and the uncertainty in the $E_{\rm c.m.}$ resolution. We add in quadrature the contributions of the various sources to determine the total systematic uncertainties.

To study the resonant substructure of the $\Upsilon(6S) \to h_b(nP)\pi^+\pi^-$ transitions, we combine the data samples of the five highest-energy points. The corresponding $M_{\rm miss}(\pi\pi)$ spectra are fitted using the same procedure as described above (see Figs. 2 and 3). The $h_b(nP)$ signal density functions are determined by averaging over the data samples that are combined; we use weights proportional to the integrated luminosity and the cross section at each

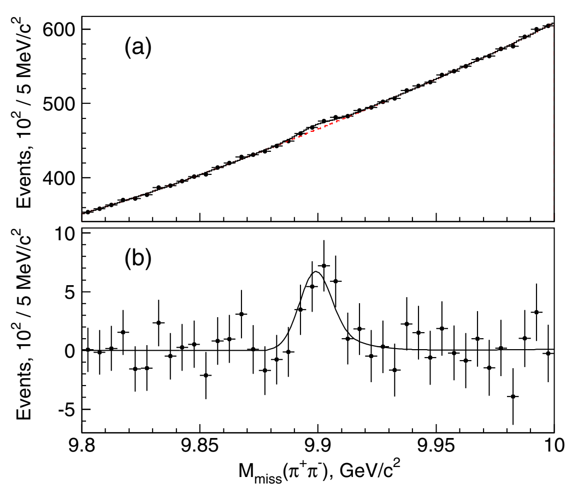


FIG. 2. The $M_{\rm miss}(\pi\pi)$ spectrum in the $h_b(1P)$ region for the combined data samples of five energy points near the $\Upsilon(6S)$. In (a), the data are the points with error bars with the fit function (solid curve) and background (red dashed curve) overlaid. (b) shows the background-subtracted data (points with error bars) with the signal component of the fit overlaid (solid curve).

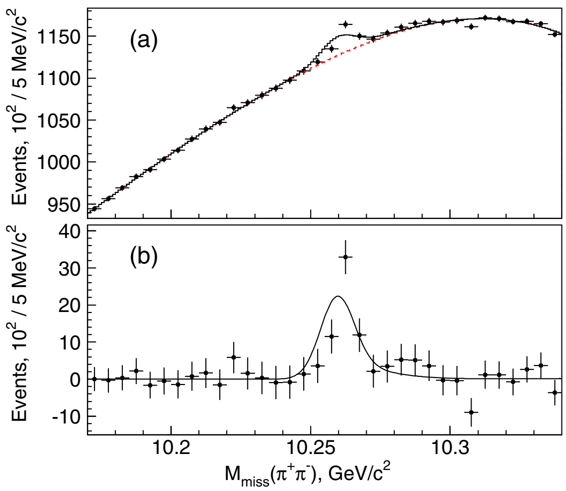


FIG. 3. The $M_{\rm miss}(\pi\pi)$ spectrum in the $h_b(2P)$ interval for the combined data samples of five energy points near the $\Upsilon(6S)$. The legend is the same as in Fig. 2.

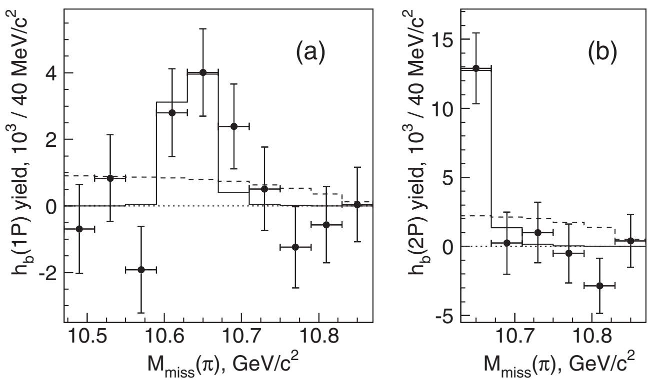


FIG. 4. The efficiency-corrected yields of $h_b(1P)\pi^+\pi^-$ (a) and $h_b(2P)\pi^+\pi^-$ (b) as functions of $M_{\rm miss}(\pi)$ for the combined data samples of five energy points in the $\Upsilon(6S)$ region. Points represent data; the solid histogram represents the fit result with the $Z_b$ signal shape fixed from the $\Upsilon(5S)$ analysis; the dashed histogram represents the result of the fit with a phase space distribution.

energy. We note that the $h_b(1P)$ and $h_b(2P)$ peaks are shifted by about 2.5 MeV/$c^2$, and the width of the $h_b(2P)$ peak is narrower by $1.2\sigma$ compared to the fit. The shift could be due to a miscalibration of the c.m. energy and is accounted for in the systematic uncertainty. The narrow width is likely a statistical fluctuation. The confidence levels of the fits are 50% and 52%, respectively. From Wilks' theorem [25], we find that the significances of the $h_b(1P)$ and $h_b(2P)$ signals are $3.5\sigma$ and $5.3\sigma$, respectively, including systematic uncertainty, determined by varying the polynomial order. Thus, we find the first evidence for the $\Upsilon(6S)\to h_b(1P)\pi^+\pi^-$ transition and observe for the first time the $\Upsilon(6S)\to h_b(2P)\pi^+\pi^-$ transition.

We release the requirement of an intermediate $Z_b$ and fit the $M_{\rm miss}(\pi\pi)$ spectra in bins of $M_{\rm miss}(\pi)$ to measure the $h_b(nP)\pi^+\pi^-$ yields as functions of $M_{\rm miss}(\pi)$. The distribution of the phase-space-generated signal events in the $M_{\rm miss}(\pi^+)$ vs $M_{\rm miss}(\pi^-)$ plane has the shape of a narrow slanted band; each structure at high values of $M_{\rm miss}(\pi^\pm)$ produces a "reflection" at small values of $M_{\rm miss}(\pi^\mp)$. We combine the $M_{\rm miss}(\pi\pi)$ spectra for the corresponding $M_{\rm miss}(\pi^+)$ and $M_{\rm miss}(\pi^-)$ bins and consider the upper half of the available $M_{\rm miss}(\pi)$ range. Thereby, we consider all signal events and avoid double counting. The yields, corrected for the reconstruction efficiencies, are shown in Fig. 4. The data are not distributed uniformly in phase space; they populate the $Z_b(10610)$ and $Z_b(10650)$ mass region. We fit the data to a shape where the $Z_b(10610)$ and $Z_b(10650)$ parameters are fixed to the $\Upsilon(5S)\to Z_b\pi\to h_b(1P)\pi^+\pi^-$ result and the nonresonant contribution is set to zero [14]. Such a model describes the data well: The confidence levels of the fits are 65% and 77% for the $h_b(1P)$ and $h_b(2P)$, respectively. The phase space hypothesis is excluded relative to this model at the $3.6\sigma$ and $4.5\sigma$ levels in the $h_b(1P)\pi^+\pi^-$ and $h_b(2P)\pi^+\pi^-$ channels, respectively. The single $Z_b(10610)$ hypothesis is excluded at the $3.3\sigma$ level in the $h_b(1P)\pi^+\pi^-$ channel, while the single $Z_b(10650)$ hypothesis cannot be excluded at a significant level. In the $h_b(2P)\pi^+\pi^-$ channel, the $Z_b(10610)^\pm$ and $Z_b(10650)^\pm$ signals overlap with the $Z_b(10650)^\mp$ and $Z_b(10610)^\mp$ reflections, respectively, which obscures the determination of the relative yields. The exclusion levels are determined using pseudoexperiments from the $\chi^2$ differences of the two hypotheses being compared and include systematic uncertainty.

In conclusion, we have measured the energy dependence of the $e^+e^-\to h_b(nP)\pi^+\pi^-$ ($n=1,2$) cross sections. We find two peaks corresponding to the $\Upsilon(5S)$ and $\Upsilon(6S)$ states and measure their parameters, which agree with the results from Ref. [11]. The data are consistent with no continuum contribution.

We report the first evidence for $\Upsilon(6S)\to h_b(1P)\pi^+\pi^-$ and the first observation of the $\Upsilon(6S)\to h_b(2P)\pi^+\pi^-$ transitions. We study their resonant substructures and find evidence that they proceed entirely via the intermediate isovector states $Z_b(10610)$ and $Z_b(10650)$. Their relative fraction is loosely constrained by the current data: The hypothesis that only $Z_b(10610)$ is produced is excluded at the $3.3\sigma$ level, while the hypothesis that only $Z_b(10650)$ is produced is not excluded at a significant level.

The shapes of the $e^+e^-\to h_b(nP)\pi^+\pi^-$ and $e^+e^-\to\Upsilon(nS)\pi^+\pi^-$ cross sections look similar. The only significant difference is a smaller relative yield of $\Upsilon(nS)\pi^+\pi^-$ at the $\Upsilon(6S)$. Since the $h_b(nP)\pi^+\pi^-$ final states are produced only via intermediate $Z_b$ while $\Upsilon(nS)\pi^+\pi^-$ at the $\Upsilon(5S)$ are produced both via $Z_b$ and nonresonantly, this difference indicates that the nonresonant contributions in $\Upsilon(nS)\pi^+\pi^-$ are suppressed at the $\Upsilon(6S)$.

We thank the KEKB group for excellent operation of the accelerator; the KEK cryogenics group for efficient solenoid operations; and the KEK computer group, the NII, and PNNL/EMSL for valuable computing and SINET4 network support. We acknowledge support from MEXT, JSPS, and Nagoya's TLPRC (Japan); ARC (Australia); FWF (Austria); NSFC and CCEPP (China); MSMT (Czechia); CZF, DFG, EXC153, and VS (Germany); DST (India); INFN (Italy); MOE, MSIP, NRF, BK21Plus, WCU, and RSRI (Korea); MNiSW and NCN (Poland); MES, RFAAE, and RSF under Grant No. 15-12-30014 (Russia); ARRS (Slovenia); IKERBASQUE and UPV/EHU (Spain); SNSF (Switzerland); MOE and MOST (Taiwan); and DOE and NSF (USA).

[1] N. Brambilla *et al.*, Eur. Phys. J. C **71**, 1534 (2011).
[2] S. K. Choi *et al.* (Belle Collaboration), Phys. Rev. Lett. **91**, 262001 (2003).
[3] K. A. Olive *et al.* (Particle Data Group), Chin. Phys. C **38**, 090001 (2014).
[4] J. P. Lees *et al.* (*BABAR* Collaboration), Phys. Rev. D **86**, 051102 (2012); Z. Q. Liu *et al.* (Belle Collaboration), Phys. Rev. Lett. **110**, 252002 (2013).
[5] J. P. Lees *et al.* (*BABAR* Collaboration), Phys. Rev. D **89**, 111103 (2014); X. L. Wang *et al.* (Belle Collaboration), Phys. Rev. D **91**, 112007 (2015).
[6] X. L. Wang *et al.* (Belle Collaboration), Phys. Rev. D **87**, 051101 (2013); M. Ablikim *et al.* (BESIII Collaboration), Phys. Rev. D **91**, 112005 (2015).
[7] M. Ablikim *et al.* (BESIII Collaboration), Phys. Rev. Lett. **111**, 242001 (2013); C. Z. Yuan, Chin. Phys. C **38**, 043001 (2014).
[8] N. Brambilla *et al.*, Eur. Phys. J. C **74**, 2981 (2014).
[9] S. Dubynskiy and M. B. Voloshin, Phys. Lett. B **666**, 344 (2008).
[10] K.-F. Chen *et al.* (Belle Collaboration), Phys. Rev. D **82**, 091106 (2010).
[11] D. Santel *et al.* (Belle Collaboration), Phys. Rev. D **93**, 011101 (2016).
[12] M. B. Voloshin, Phys. Rev. D **85**, 034024 (2012).
[13] I. Adachi *et al.* (Belle Collaboration), Phys. Rev. Lett. **108**, 032001 (2012).
[14] A. Bondar *et al.* (Belle Collaboration), Phys. Rev. Lett. **108**, 122001 (2012).
[15] A. E. Bondar, A. Garmash, A. I. Milstein, R. Mizuk, and M. B. Voloshin, Phys. Rev. D **84**, 054010 (2011).
[16] A. Abashian *et al.* (Belle Collaboration), Nucl. Instrum. Methods Phys. Res., Sect. A **479**, 117 (2002); also see detector section in J. Brodzicka *et al.*, Prog. Theor. Exp. Phys. **2012**, 04D001 (2012).
[17] S. Kurokawa and E. Kikutani, Nucl. Instrum. Methods Phys. Res., Sect. A **499**, 1 (2003), and other papers included in this volume; T. Abe *et al.*, Prog. Theor. Exp. Phys. **2013**, 03A001 (2013), and references therein.
[18] R. Mizuk *et al.* (Belle Collaboration), Phys. Rev. Lett. **109**, 232002 (2012).
[19] K. Abe *et al.* (Belle Collaboration), Phys. Rev. D **64**, 072001 (2001).
[20] G. C. Fox and S. Wolfram, Phys. Rev. Lett. **41**, 1581 (1978).
[21] E. A. Kuraev and V. S. Fadin, Sov. J. Nucl. Phys. **41**, 466 (1985); M. Benayoun, S. I. Eidelman, V. N. Ivanchenko, and Z. K. Silagadze, Mod. Phys. Lett. A **14**, 2605 (1999).
[22] A. Garmash *et al.* (Belle Collaboration), Phys. Rev. D **91**, 072003 (2015).
[23] S. Actis *et al.*, Eur. Phys. J. C **66**, 585 (2010).
[24] See Supplemental Material at http://link.aps.org/supplemental/10.1103/PhysRevLett.117.142001for tables of $\sigma^B[e^+e^- \to h_b(nP)\pi^+\pi^-]$ ($n = 1$, 2) measurements.
[25] S. S. Wilks, Ann. Math. Stat. **9**, 60 (1938).